American Journal of Engineering and Applied Sciences

Original Research Paper

Study of Concentrated Solar Power Collectors with Organic Rankine Cycle and Magnetized Nanofluids

Samuel Sami Howard

TransPacific Energy, Inc., Las Vegas, NV 89183, USA IES, University of North Dakota, Grand Forks, ND, 58202

Article history
Received: 25-01-2022
Revised: 10-02-2022
Accepted: 11-02-2022

Email: dr.ssami@transpacenergy.com

Abstract: The performance of "magnetized nanofluids in a Parabolic Trough Concentrating Solar Collector (CSP)-integrated Organic Rankine Cycle (ORC) and a Thermal Energy Storage (TES) systems are studied. The characteristics of magnetized nanofluids AI_2O_3, CuO, $Fe_3O_{4,\ and}$ SiO_2 as heat transport fluid circulating in integrated Concentrating Solar Power (CSP) with ORC and TES under different solar radiations, angles of incidence, and different nanofluid concentrations have been presented. An environmentally refrigerant quaternary was used in the ORC loop to enhance the ORC efficiency composed of R1234ze, R245fa, R125, and R236fa was used. The results showed that the power absorbed and collected by the CSP collector and thermal energy stored is enhanced with the increase of solar radiation. It was also observed that the CSP hybrid system efficiency has been enhanced mainly by the increase of solar radiations, higher magnetized nanofluid concentrations, and the magnetic fields over the thermal oil as base fluid. Also, the study concluded that the nanofluid CuO outperformed the other nanofluids-Al_2O_3, $Fe_3O_{4,\ and}$ SiO_2-at similar conditions. Finally, it was found that the model's prediction compared fairly with data reported in the literature; however, some discrepancies existed between the model's prediction and the experimental data".

Keywords: CSP Solar Collectors, Magnetized Nanofluids, Organic Rankine Cycle, Modeling, Simulation and Model's Validation

Introduction

As energy demand across the globe increases, harnessing renewable energy remains essential to combat global warming and climate change. "Concentrating sunlight is an effective way to generate higher output and magnetized nanofluids can play a crucial role in the development of these technologies. Solar energy can be utilized to produce both electricity and heat. Thermal storage integrated CSPs overcome the intermittency of solar radiation. The thermophysical properties of the Heat Transfer Fluids (HTF) and the Thermal Energy Storage (TES) materials are key to enhancing the system's efficiency. A stable nanofluid retains its optical and thermal properties and can be subjected to several destabilizing factors. Understanding these factors is crucial for designing and selecting a stable nanofluid. The CSP uses solar concentrators to focus solar radiation onto a receiver that carries a heat transfer fluid that is heated to a high temperature. Generally, in most CSP plants, the heat transfer fluid is thermal oil. In this study, this heat transfer fluid goes to an Organic Rankine Turbine generator (ORC), where power is generated".

Reviews of different "Concentrated Solar Power (CSP) collectors' applications have been reported in the literature. however, a possible improvement of CSP technologies can be realized through integration into a hybrid system that uses nanofluid heat transport fluid to drive the Organic Rankine Cycle (ORC) system. This simultaneously provides heat and power (Pavlović *et al*., 2012; Ummadisingu and Soni, 2011; Izquierdo *et al*., 2010; Paces, 2016; Mohamad *et al*., 2014; Islam *et al*., 2018; Peters *et al*., 2011; Macchi and Astolfi, 2016; Freeman *et al*., 2017; Taylor *et al*., 2011; Nagarajan *et al*., 2014; Calise and Vanoli, 2012; Bozorgan and Shafahi, 2015; Shin *et al*., 2010; Lomascolo *et al*., 2015; Milanese *et al*., 2016; Iacobazzi *et al*., 2016; Bahram *et al*., 2013; Tzivanidis *et al*., 2016; Alashkar and Gadalla, 2018; Saloux *et al*., 2019; Sami and Marin, 2016; Sami, 2011; Silva and Castro, 2012; Sharma *et al*., 2017; Sami, 2019; SRD, 2013; Boonrit, 2017; Sami and Marin, 2019; Sami, 2019; Zhang *et al*., 2019; Marefati *et al*., 2018; Wang *et al*., 2019; Dickes *et al*., 2014; Saadatfar *et al*., 2014; Bellos and Tzivanidis, 2017; Incropera and DeWitt, 1994; HTFDC, 2022; Czaplicka *et al*., 2021; Xu *et al*.,

2015; Bellos *et al*., 2016). Thermal energy storage is an integral part of a CSP plant to overcome the intermittency of solar radiations for continuous production of power during the night and on cloudy days" (Macchi and Astolfi, 2016; Freeman *et al*., 2017).

A detailed review was reported by Czaplicka *et al*. (2021) on the novel "nanoparticle-based materials used as heat transfer fluids and in-depth comparison of environmental, technical and economic characteristics of the thermophysical properties including thermal conductivity, specific heat, density, viscosity, and Prandtl number. Also, the review discussed the possible benefits and limitations of various transfer fluids in the fields of application where the efficiency of heat transfer to heat transport fluid is important. It has been shown theoretically and experimentally that, in low-temperature solar collectors at around 100°C, efficiency can be improved by using nanofluids" (Taylor *et al*., 2011; Nagarajan *et al*., 2014).

The enhancement of the "thermal properties of various high-temperature nanofluids for solar thermal energy storage application in Concentrating Solar Power (CSP) systems, the thermophysical properties of the Heat Transfer Fluids (HTF) and the Thermal Energy Storage (TES) materials were studied, and presented by (Shin *et al*., 2010) where the silica (SiO_2) and alumina (Al_2O_3) nanoparticles, as well as Carbon Nanotubes (CNT), were dispersed into molten salt. Dimensional analyses and computer simulations were performed to predict the enhancement of thermal properties of the nanofluids".

Tzivanidis *et al*. (2016) reported and analyzed "high-temperature Parabolic Trough Collectors (PTC) coupled with an Organic Rankine Cycle (ORC) to carry out optimization at both levels: Financially and energetically. They investigated the solar field, the storage tank, and the ORC module under many conditions of collecting solar areas and storage tank volumes." They also presented an economic comparison for different commercial solar collectors.

Alashkar and Gadalla (2018) studied "the performance of Parabolic Trough Solar Collector (PTSC)-based power generation plant, the effect of adding an Organic Rankine Cycle (ORC) and a Thermal Energy Storage (TES) system and the most efficient fluid on the performance and financial metrics of the PTSC-power plant. The simulation results showed that Benzene is the most efficient organic fluid, having the highest thermal and energetic efficiency and the lowest pumping power when compared to other organic fluids. Finally, thermodynamic modeling of ORC was reported in the literature by Saloux *et al*. (2019), Sami and Marin (2016; Sami, 2011), and Silva and Castro (2012) where low- and high-grade waste heat is converted into power".

The literature review demonstrated that research reported in the literature was only focused on "ORC is driven by thermal oil heat transport fluids and rarely by nanofluids fluids The potential and advantages of using nanofluids were found to enhance the thermodynamic efficiencies under optimum conditions and higher than those obtained from the base fluid. Further, the size of heat exchangers, evaporators, and condensers is lower than those using the base fluid. However, none was reported on magnetized nanofluids thermal oil-based driving ORCs". Therefore, this study is considered a new contribution to the ORCs driven by magnetized nanofluids.

In this study, a "simulation numerical model was presented to study the "behavior of the different magnetized nanofluids circulating in the parabolic trough solar collector to drive an Organic Rankine Cycle, under different solar radiations. The model was based upon the mass and energy equations written for the heat transport fluid with magnetized nanofluids. These equations were integrated and solved using the finite difference method to predict the behavior of the Parabolic Trough Collectors (PTC) driving an Organic Rankine Cycle (ORC) under different operating conditions such as solar radiations, magnetized nanofluid flow rates, ambient temperatures, magnetic field, and various volumetric nanofluid concentrations". This study was intended to investigate the "enhancement and "characteristics of magnetized nanofluids AI_2O_3 CuO, Fe_3O_4 and SiO_2 in an integrated Concentrating Solar Power (CSP) with ORC and Thermal Storage (TES) under different solar radiations, angle of incidence and different magnetized nanofluids concentrations and magnetic fields This research represents a significant contribution to the nanofluid science where nanofluid is used to enhance the performance of CSP solar collectors and integrated ORCs compared to thermal oil as base heat transport fluid".

Mathematical Model

The mathematical model was established based on the "mass and energy equations written to describe the behavior of the nanofluids driving an Organic Rankine Cycle, ORC, with a refrigerant mixture" as shown in Fig. 1. This figure depicts the proposed CPS system. "The CPS thermal loop is composed of a CPS solar collector, thermal storage tank, and pump, as well as the waste heat boiler of the ORC. The solar radiation is absorbed by the CSP solar collector and converted into thermal energy that heats the nanofluids and thermal oil circulating in the thermal oil/storage tank loop. The thermal oil is the base fluid heat transport fluid with nanofluids is used to drive the ORC circuit".

The thermal storage tank is used to store "thermal energy and during the intermittent solar radiation periods, it supplies heat to the ORC waste heat boiler. In the ORC circuit, the thermal heat absorbed evaporates the refrigerant mixture that drives the turbine. In the turbine, the thermal energy is converted into kinetic energy and produces power at the turbine shaft and the generator. The

DOI: 10.3844/ajeassp.2022.101.117

low-pressure vapor is condensed in the condenser into liquid and pumped back to the waste heat boiler. The refrigerant mixture used in the ORC loop is an environmentally sound quaternary mixture composed of R134a, R245fa, R125, R236fa" (Sami, 2011). Thermodynamic and thermophysical properties were obtained at REFPROP (SRD. 2013). Figure 2 depicts the "thermodynamic properties and the pressure-enthalpy diagram of the mixture R134a, R245fa, R125, R236fa, where it is quite clear that one of the most important characteristics is the variable saturation temperature and glide temperature". This feature is pivotal in enhancing the Organic Rankine Cycle efficiency.

In the following sections, the different "equations of mass and energy are presented. It is assumed in the model that the nanofluid is homogeneous, isotropic, incompressible, and Newtonian; that inlet velocity and inlet temperature are constant; and that the thermophysical properties of the nanofluids" are constant. In the following, the conservation mass and energy equations and heat transfer equations are written and presented for each element of the nanofluids.

CSP Solar Collector Model

The power absorbed from solar radiation by the CSP solar collector can be determined by the following (Izquierdo *et al*., 2010; Paces. 2016; Mohamad *et al*., 2014; Islam *et al*., 2018; Sami, 2011):

$$P_{abs} = DIN * \cos\theta * \eta_{opt} * IAM * R_s * E_L * SF_{Avail} \quad (1)$$

where,

DNI: Solar radiation (w/m^2)
Θ: Angle of incidence
η_{opt}: Optical efficiency
IAM: Incidence angle modifier.
R_s: Row shadow
E_l: End losses
SF_{Aval}: Solar field available

The CSP collected power is given by:

$$P_{collector} = P_{abs} - P_{losscol} - P_{losspip} \quad (2)$$

where:
P_{abs}: Collector power absorbed by CSP defined in Eq. (1)
$P_{losscol}$: Collector thermal losses of the CSP.
$P_{losspip}$: Solar field piping losses.

The collected power calculated in Eq. (2) is transferred to the "heat transfer fluid, thermal oil, and nanofluids loop. It is also assumed that this thermal energy will be accumulated in the thermal storage tank that supplies the thermal energy to drive the ORC cycle".

The CSP collector thermal losses are calculated by Eq. (3)–(5):

$$P_{losscol} = L_{c1} + L_{c2} \quad (3)$$

$$L_{c1} = a_2\Delta T_1^2 + a_1\Delta T_1 - a_0 \quad (4)$$

$$L_{c2} = \left(b_2\Delta T_1^2 + b_1\Delta T_1 - b_0\right)\left(\frac{DNI}{900}\right)\cos\theta \quad (5)$$

Readers interested in the detailed calculation of the collector thermal losses are advised to consult references (Izquierdo *et al*., 2010; Paces. 2016; Mohamad *et al*., 2014; Islam *et al*., 2018; Sami, 2011).

On the other hand, the piping losses are determined from the following equation:

$$P_{losspip} = L_{p1}\Delta T_1 - L_{p2}\Delta T_1^2 + L_{p3}\Delta T_1^3 \quad (6)$$

Readers interested in the detailed calculation of the collector piping losses are advised to consult (Izquierdo *et al*., 2010; Paces. 2016; Mohamad *et al*., 2014; Islam *et al*., 2018; Sami, 2011).

Finally, the power of the CSP collector is:

$$P_{collector} = P_{abs} - P_{losscol} - P_{losspip} \quad (7)$$

where, Eq. (3) and (6) define the collector thermal losses $P_{losscol}$ and piping losses, $P_{losspip}$, respectively.

The mass flow rate of the basic heat transfer fluid, thermal oil, can be given by the following:

$$m_{oil} = \frac{P_{collector}A_{aperture}}{C_{p_{oil}}\left(T_{field_{outlet}} - T_{field_{inlet}}\right)} \quad (8)$$

where,

$A_{aperture}$ = The total aperture (m^2)
$T_{field\ outlet}$ and $T_{field\ inet}$ = The outlet and inlet temperature of the thermal oil in the solar field

The "Dowtherm fluid was used in this CSP loop since it offers good thermal stability at temperatures up to 625°F (330°C). The maximum recommended film temperature is 675°F (360°C). Between 550 and 600°F (290 and 315°C), its stability is 15 to 30 times greater than that of a typical hot oil. Where the specific heat of the thermal oil" is (Incropera and DeWitt, 1994):

$$C_{p_{oil}} = 1509 + 2.496T_{oil} + 7.887 * 10^{-4}T_{oil}^2 \quad (9)$$

where T_{oil} is the thermal *oil* temperature.

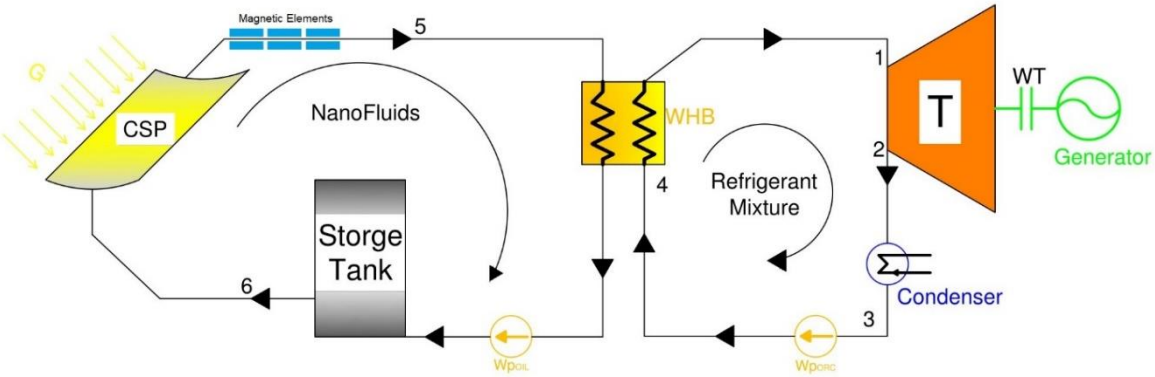

Fig. 1: Flow diagram of the proposed magnetized CSP system

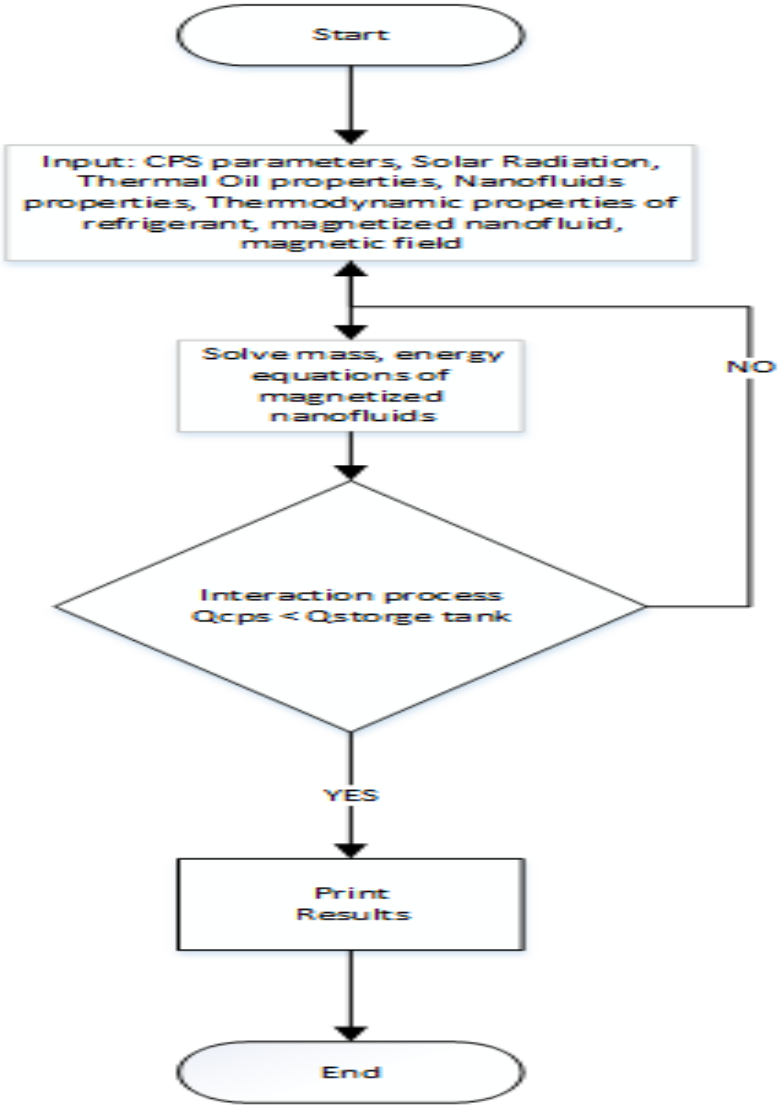

Fig. 2: Logical diagram for the numerical model

DOI: 10.3844/ajeassp.2022.101.117

The thermal heat accumulated in the thermal storage tank during the charging process is:

$$Qstoragetank = \eta m_{oil}\left(T_5 - T_6\right)C_{p_{oil}} \tag{10}$$

where m_{oil} is the oil flow rate obtained from Eq. (8) and C_{poil} is the specific heat of thermal oil in the base fluid.

The thermal heat during the discharging process is (Zhang *et al*., 2019):

$$\begin{aligned} Qstoragetank &= m_{oil}\left(T_{hot\,tank} - T_{cold\,tank}\right)C_{p_{oil}} \\ &= \eta\, m_{salt}\left(T_{hot\,tank} - T_{cold\,tank}\right)C_{p_{salt}} \end{aligned} \tag{11}$$

m_{salt}: Mass of salt in the storage thermal tank
η : Efficiency of heat exchanger

The energy balance at the ORC cycle gives the following (Sami, 2011):

$$W_{ORC} = m_{ref}\left(h_1 - h_2\right) \tag{12}$$

$$Q_{WHB} = m_{ref}\left(h_1 - h_4\right) \tag{13}$$

$$Q_{COND} = m_{ref}\left(h_2 - h_3\right) \tag{14}$$

$$W_{P_{ORC}} = m_{ref}\left(h_4 - h_3\right) \tag{15}$$

where,

h_1: Enthalpy at the outlet of the waste heat boiler (kj/Kg)
h_2: Enthalpy at the exit of the vapor turbine (kj/Kg)
h_3: Enthalpy at the condenser outlet (kj/kg)
h_4: Enthalpy at ORC pump outlet (kj/kg)
m_{ref}: Refrigerant mass flow rate (kg/s)

An "environmentally sound quaternary refrigerant with low GWP was used in the ORC cycle and its enthalpies and entropies, as well as its thermal properties", were calculated using the REFPROP program and EES (Sami, 2011; Silva and Castro, 2012; Sharma *et al*., 2017; Sami, 2019a; SRD, 2013; Boonrit, 2017; Sami and Marin, 2019; Sami, 2019b; Xiaoming *et al*., 2019; Marefati *et al*., 2018) for the refrigerant blend under investigation.

The ORC efficiency can be calculated as:

$$\eta_{ORC} = \frac{W_{ORC} - W_{P_{ORC}}}{Q_{WHB}} \tag{16}$$

where,

W_{ORC} and W_{PORC}: Represent the work produced by the ORC and the work used by the ORC pump
Q_{WHB}: Thermal energy supplied by the waste heat boiler

$$\eta_{CSP} = \frac{Qabs}{Q_{CSP}} \tag{17}$$

where,

W_{poil} = Work used by the thermal *oil* pump
Q_{CSP} = The CSP power collected and defined by Eq. (1).

Finally, the hybrid system efficiency is:

$$\eta_{SH} = \frac{W_{ORC} - W_{P_{ORC}} - W_{P_{oil}}}{Q_{ecllector}} \tag{18}$$

where $Q_{collector}$ represents the collected CSP power and is given by Eq. (2).

The hybrid system refers to the CSP collector, thermal oil loop, and the ORC cycle.

Nanofluid Heat Transfer Fluid

The basic heat transport fluid in the CPS loop is thermal *oil*. However, nanofluids have been added to the thermal oil to enhance its thermal properties. Sharma *et al*. (2017), Sami (2019a-b) and Marefati *et al*. (2018) presented equations to calculate the "thermophysical and thermodynamic properties of nanofluids such as specific heat, thermal conductivity, viscosity, and density, employing the law of mixtures as a function of the volumetric concentration of nanoparticles";

$$\alpha_{total} = \alpha_{particles} + \alpha_{base\ fluid} \tag{19}$$

where α represents a particular thermophysical property of the nanofluid under investigation.

The nanofluid thermal and thermophysical properties, α_{total}, can be calculated as follows:

$$\alpha_{total} = \alpha_{base\ fluid} + \alpha_{particles}\left(\Phi\right) \tag{20}$$

where Φ represents the nanoparticle's volumetric concentration.

The thermal conductivity is related to thermal diffusivity and density of the nanofluids as follows:

$$\lambda = \alpha\delta C_p \tag{21}$$

where C_p is the specific heat, α is the thermal diffusivity, and λ and ρ represent the thermal conductivity and density, respectively.

The specific heat is calculated for nanofluids as follows (Sharma *et al*., 2017; Sami, 2019a; SRD, 2013; Boonrit, 2017; Sami and Marin, 2019; Sami, 2019b):

$$C_{pnf} = \frac{\left(1-\phi\right)\left(\rho C_p\right)b_f + \phi\left(\rho C_p\right)_p}{\left(1-\phi\right)\rho_{bf} + \phi\rho_p} \tag{22}$$

Table 1: Thermophysical Properties of magnetized nanofluids

	Ai203	CuO	Fe304	SiO_2
C_{pnf}	b = 0.1042a+6226.5	b = 0.2011a+5730.8	b = 0.8318a+4269.8	b = 0.6187a+4293.2
K_{nf}	b = 2E-05a+1.4888	b = 5E-05a+1.3703	b = 0.0002a+1.0209	b = 0.0001a+1.0265
h	b = 0.0031a+73.092	b = 0.0031a+73.073	b = 0.003a+73.225	b = 0.003a+73.231

where "*nf*" and "*bf*" refer to nanofluid and basic fluid, respectively. *Ø* is the nanofluid particle concentration. ρ represents the density.

The density of nanofluids can be written as follows (Sharma *et al*., 2017; Sami, 2019a; Zhang *et al*., 2019):

$$\rho_{nf} = \phi_p \rho_p + (1-\phi)\rho_{bf} \quad (23)$$

ρ_p represents the density of the nanoparticle.

Magnetized Nanaolfuids:

Equations (13) through (15) can be used to determine other "thermophysical properties such as; α is the thermal diffusivity, ʎ and ρ represent the thermal conductivity and density as different magnetic forces Gauss published in the literature properties (Freeman *et al*., 2017; Taylor *et al*., 2011; Alashkar and Gadalla, 2018) as a function of the properties" outlined in Table 1.
where "b" represents the nanofluid-specific property and "a" is the magnetic field force in Gauss. C_{pnf}, $K_{nf,\ and}$ h are the specific heat, thermal conductivity, and heat transfer coefficients of nanofluids.

Numerical Procedure

Figure 2 describes the sequence of steps and calculations of the numerical model in question describing the "energy conversion mechanisms taking place during energy conversion in the CSP, thermal oil loop, and the ORC cycle" presented in Eq. (1)–(23). The logical diagram presented these "equations integrated into finite-difference formulations". Iterations were performed using MATLAB iteration techniques until a converged solution is reached with an acceptable iteration error of ±0.05. The logical diagram presented in Fig. 2 starts inputting "solar radiations, magnetized nanofluids, specifications and parameters to initiate the calculation of the CSP collected power, thermal oil flow, storage tank, refrigerant flow and finally the different ORC components and work produced. To this end, the CSP, ORC, and hybrid system efficiencies were calculated'.

Discussion and Analysis

Samples of the predicted results for the "CSP, thermal oil loop, and ORC cycle were studied under different inlet conditions and are analyzed and discussed in the following sections for different solar radiations at different angles of incidence at 8 am, 12, and 4.00 pm and with different nanofluids- AI_2O_3, CuO, Fe_3O_4 and SiO_2-with a mainly thermal oil supply with exit temperatures of the CSP collector of 166.5°C (331°F) and 149.5°C (301°F), respectively and an ambient temperature of 25°C (77°F). Other output temperatures of the CSP solar collector were considered: 182°C (361°F) and 199°C (391°F)".

AI2O3 is one of the most studied nanofluids in the literature (Iacobazzi *et al*., 2016; Sami, 2919a; Sami and Marin, 2019; Sami, 2019b); Fig. 5 through Fig. 9 presented the different "characteristics of the CSP solar collector system for 5% concentrations of the magnetized nanofluid AI_2O_3. We present results in these figures for the characteristics of the CSP hybrid system, including absorbed thermal energy, thermal energy stored, thermal energy delivered to the waste heat boiler of the ORC, and finally work produced by ORC, where the thermal oil with suspended magnetized nanofluid AI_2O_3, at three different times during the day and with different angles of incidence of the solar radiation: 17.44° at 8:00 am, 77.44° at 12:00 pm and 137.44° at 16:00. Specifically, Fig. 3 displays the power absorbed by the CSP at different times during the day and at different angles of incidence in January 2018. The maximum power absorbed by the CSP occurs from midday-12:00 pm. However, the highest power was observed at 8:00 am due to the solar radiation being higher at 8:00 am compared to at 4:00 pm. On the other hand, Fig. 4 shows the predicted efficiencies produced by the ORC at different times during the day and different angles of incidence. This figure also confirms that the maximum efficiency produced by the CSP hybrid system occurs at midday. Furthermore, other main parameters of the CSP system-power absorbed, power collected, storage tank thermal energy, and work generated by the ORC at different direct normal insolation and angles of the incident have been are depicted in Fig. 3 and 4. It is quite evident from the results displayed in these figures that the higher the solar radiation, the higher the characteristics of the CSP system and the power produced by the ORC. Furthermore, the maximum efficiencies of the CSP and the hybrid system occur in mid-dia. and that can be attributed to the fact that higher solar radiation at higher angles of incidence increases the thermal energy absorbed by the CPS collector and the thermal energy delivered to the waste heat boiler of the ORC".

A discussion and analysis of the impact of the "magnetic field nanofluid of AI_2O_3 at a concentration of 5% in Fig. 5-9 on the different characteristics of the CSP collector, such as thermal energy absorbed by a solar collector, thermal energy collected, thermal energy in the

storage tank, thermal energy supplied to the waste heat boiler of ORC, work produced at the ORC's turbine and efficiencies of the CSP collector hybrid system" calculated based on Eq. (17) through (19), respectively.

Furthermore, the predicted results of the "CSP system Characteristics using magnetized nanofluid AI_2O_3 depicted in Fig. 5 through 9 have been enhanced at the higher magnetic field over the thermal oil as base fluid presented in Fig. 3 and 4 and were maximized at midday, when solar radiation is at its highest peak. Similar results were observed in the efficiencies of the CSP and the hybrid system that peaked at midday. It is also worthwhile mentioning that similar behavior was observed with other magnetized nanofluids; CuO, $Fe_3O_{4,\ and}$ SiO_2 "

Other nanofluids, such as "CuO, $Fe_3O_{4,\ and}$ SiO_2, have received significant attention in the literature, namely, (Sami, 2011; Silva and Castro, 2012; Sharma *et al*., 2017; Sami, 2019a; SRD, 2013; Boonrit, 2017; Sami and Marin, 2019; Sami, 2019b). In the following section, we will discuss the impact of using these nanofluids as heat transfer fluid in the thermal oil loop of the CSP solar collector on the characteristics of the CSP hybrid system; Fig. 9-14. It is evident from the results depicted in these figures that the magnetized nanofluids CuO and AI_2O_3 have the highest characteristic performance among the other nanofluids in the CSP solar collector system over the thermal oil as base heat transfer fluid. This can be attributed to the higher thermodynamic thermophysical and heat transfer properties of the magnetized nanofluid CuO and AI_2O_3 which contribute to outperforming other nanofluids over the base fluid thermal oil".

In particular, Fig. 11 clearly shows that the "magnetized nanofluid CuO and AI_2O_3 have the highest ORC work produced among the other nanofluids under investigation. This results in enhancing the hybrid CSP solar collector system efficiency compared to the other nanofluids under study. It has been also observed during this investigation that, in general, the higher the nanofluid concentration, the higher the hybrid system performance characteristics."

Thereafter, the "higher the concentration of the magnetized nanofluid the higher the CSP system characteristics, such as ORC performance, thermal energy at the storage tank, and thermal energy supplied to the waste heat boiler of the ORC. Also, the maximum value was achieved by midday, at which point solar radiation is at its highest, at 599.67 w/m^2 measured at the site. As expected, the results in these figures and others indicate that the higher efficiencies of the hybrid system the higher the solar radiations, but, the CSP collector efficiencies are independent of the nanofluid concentrations", as per Eq. (17).

Figure 15 depicts the variation of the "refrigerant mass flow rate of the ORC cycle at the mid-day and different angles of incidence of the solar radiation: 77.44° at midnight. The highest simulated nanofluid concentration is the highest refrigerant mass flow rate and consequently the highest the ORC output work. However, it is worthwhile pointing out that nanofluid concentration higher than 20% could result in higher pressure head losses and pumping power losses in the thermal oil loop and that is undesirable. Therefore, the designer of such systems needs to exercise caution when using a higher concentration of nanofluids (Sami, 2011; Silva and Castro, 2012; Sharma *et al*., 2017; Sami, 2019a; SRD, 2013; Boonrit, 2017; Sami and Marin, 2019; Sami, 2019b). Also is worthwhile to highlight that the data showed that up to nanofluid concentrations of 5% there is no great difference between the nanofluids in impacting the refrigerant flow rate and consequently the ORC output work."

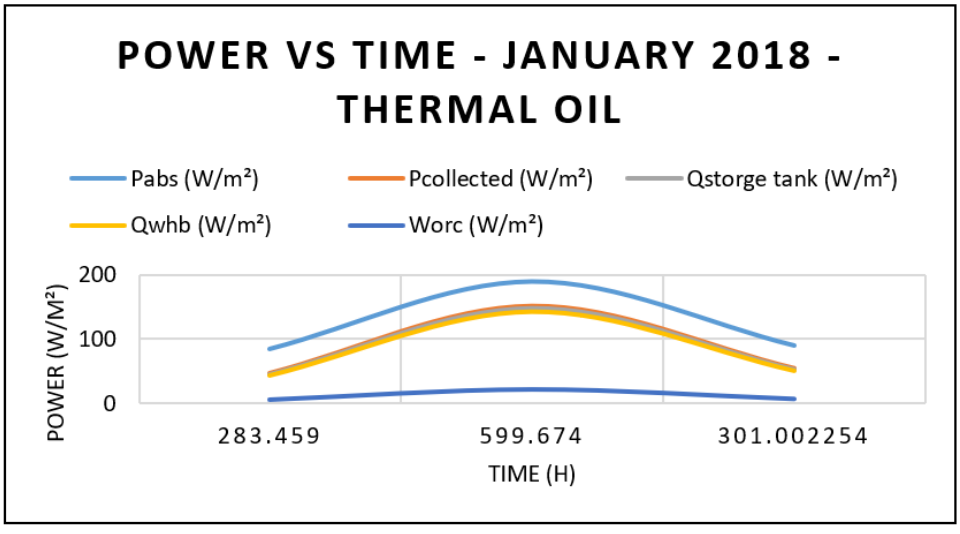

Fig. 3: CSP hybrid system results with thermal oil as base fl

DOI: 10.3844/ajeassp.2022.101.117

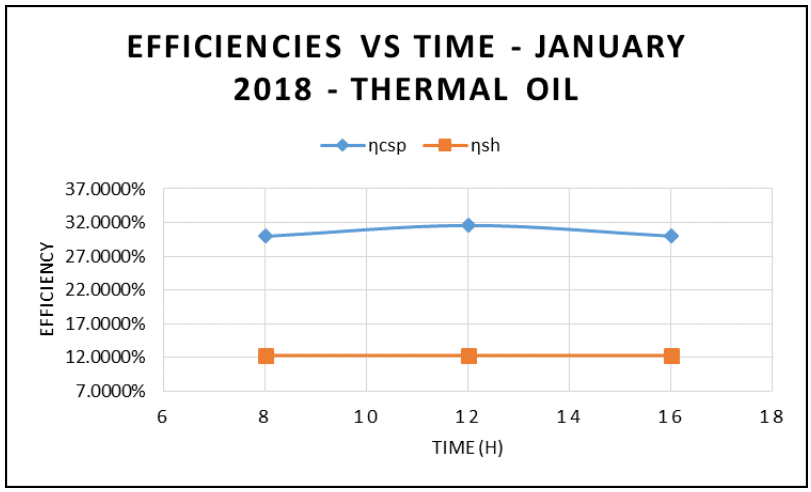

Fig. 4: The efficiency of CSP collector and hybrid system at a different angle of incidence and thermal oil as base fluid

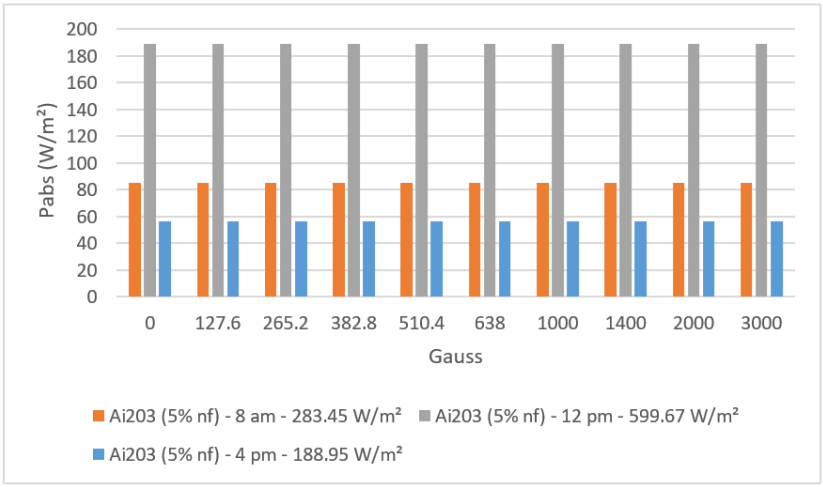

Fig. 5: Characteristics of the CSP collector and hybrid system at a concentration of 5% of AI_2O_3

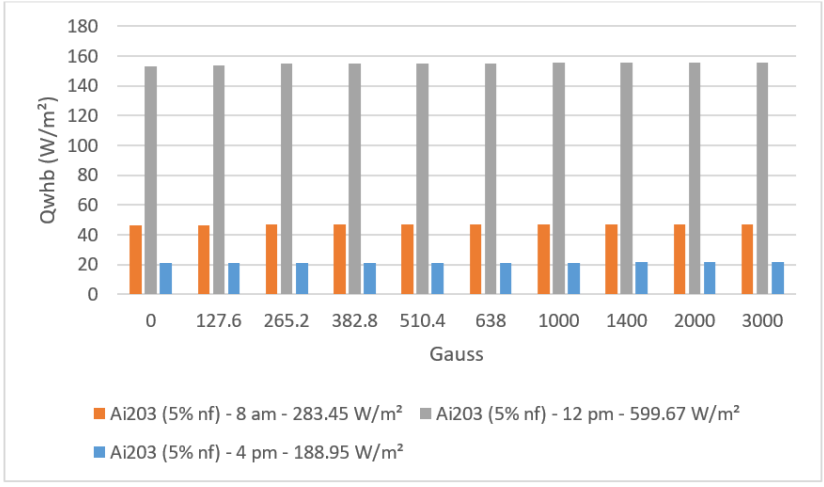

Fig. 6: Characteristics of the CSP collector hybrid system and waste heat boiler at a concentration of 5% of AI_2O_3

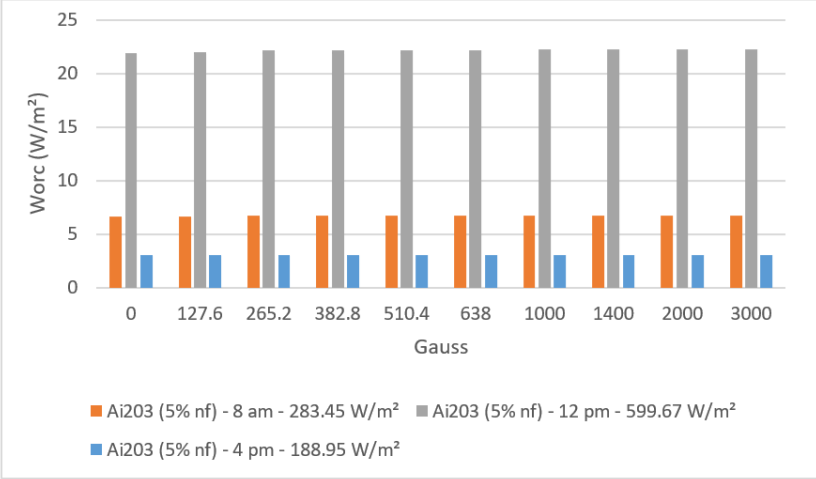

Fig. 7: Characteristics of the CSP collector hybrid system for ORC work produced at a concentration of 5% of AI_2O_3

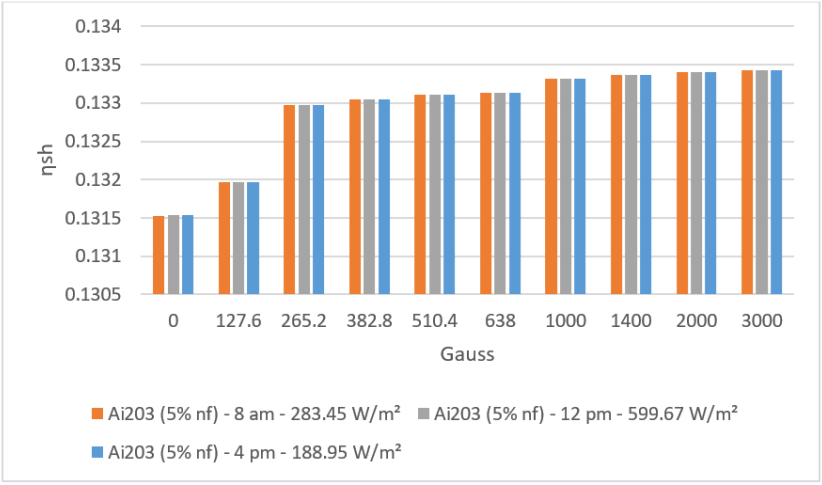

Fig. 8: Efficiencies of the CSP collector hybrid system at a concentration of 5% AI_2O_3

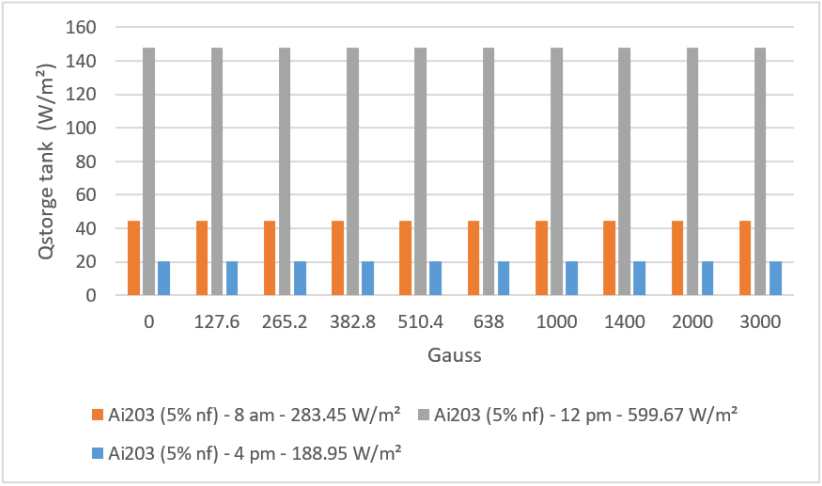

Fig. 9: Thermal storage at the CSP collector hybrid system thermal storage at a concentration of 5% AI_2O_3

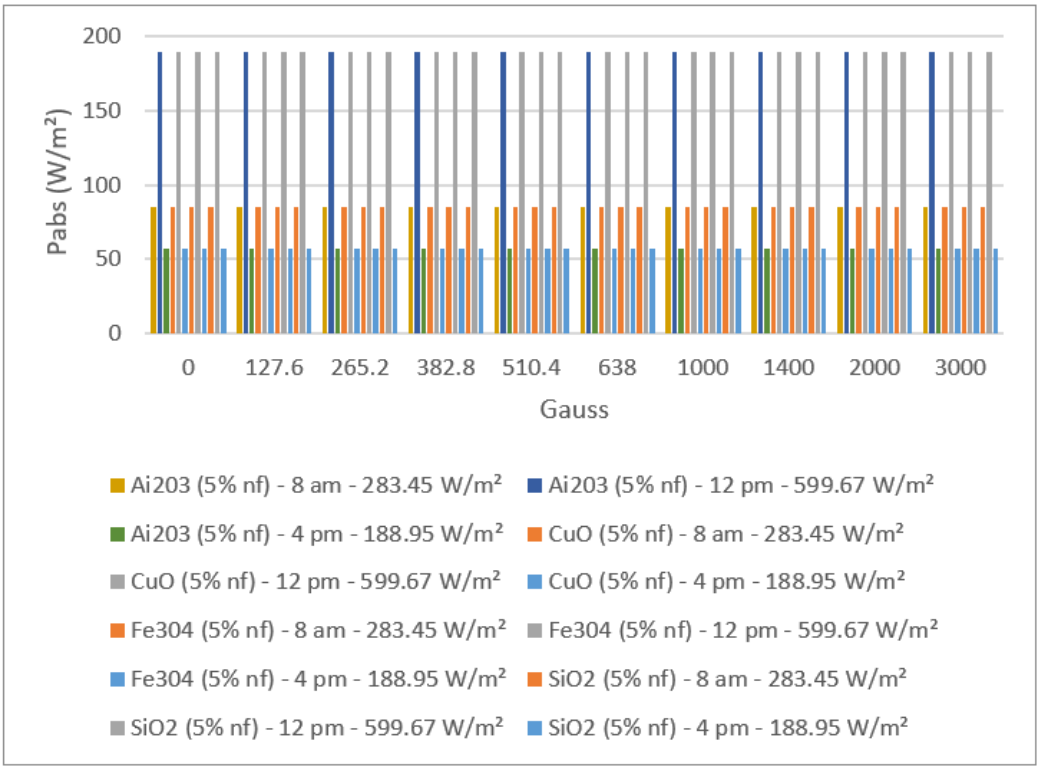

Fig. 10: CSP collector thermal energy and hybrid system at different magnetic fields

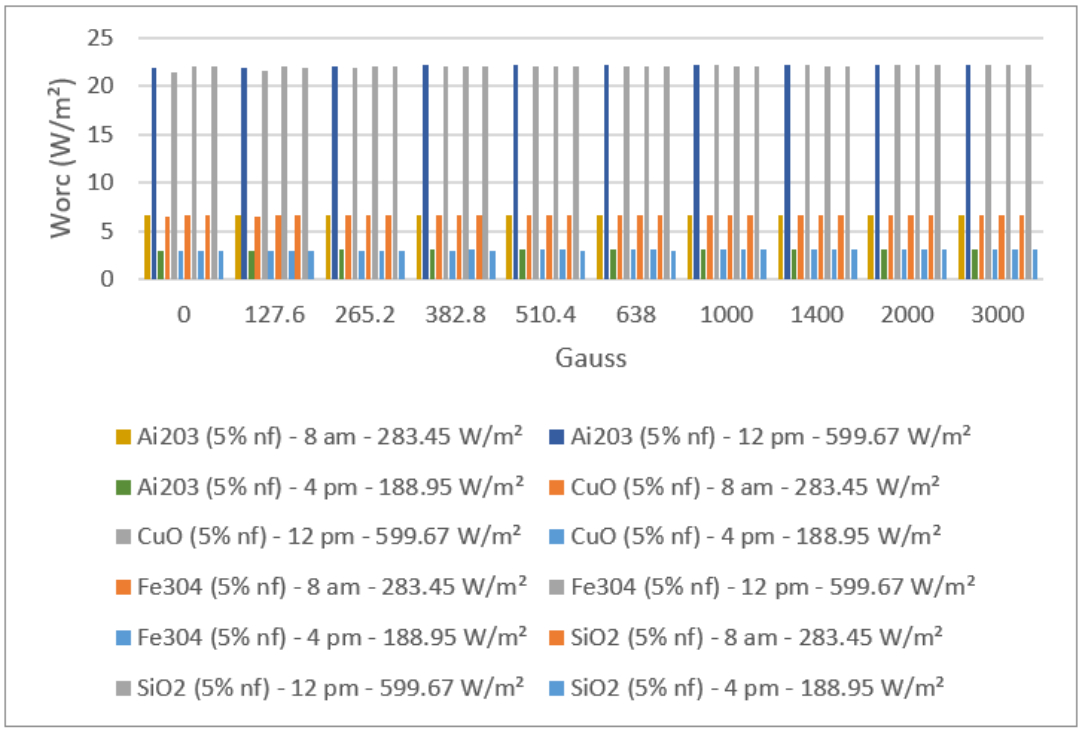

Fig. 11: ORC work in different magnetic fields

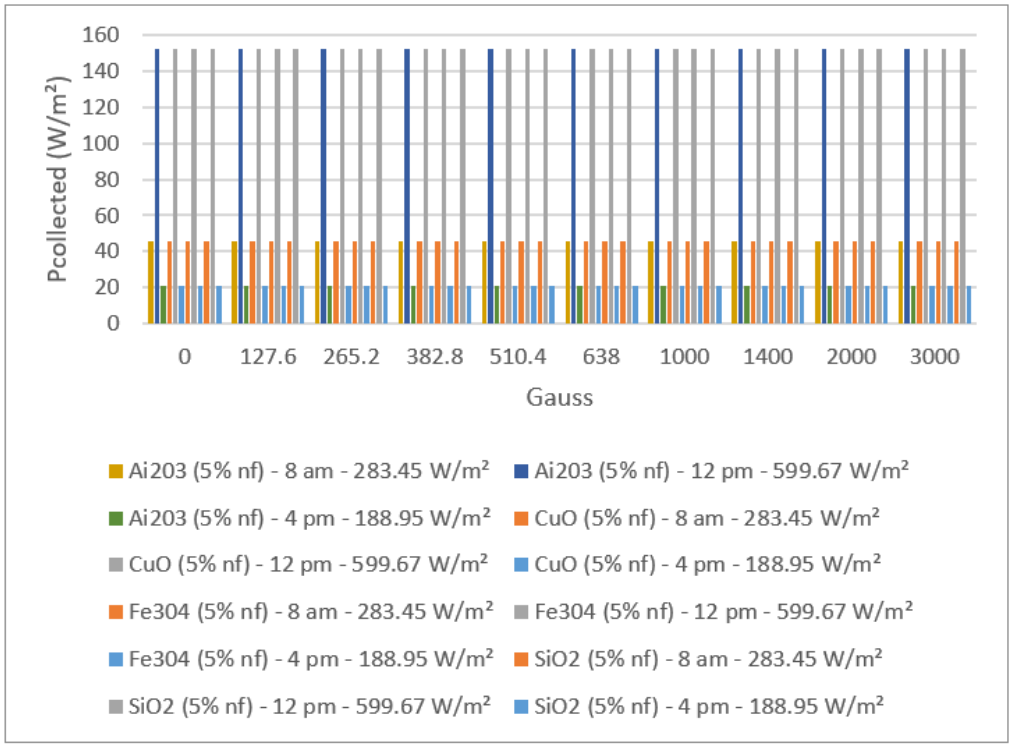

Fig. 12: CSP thermal energy collected at different magnetic fields

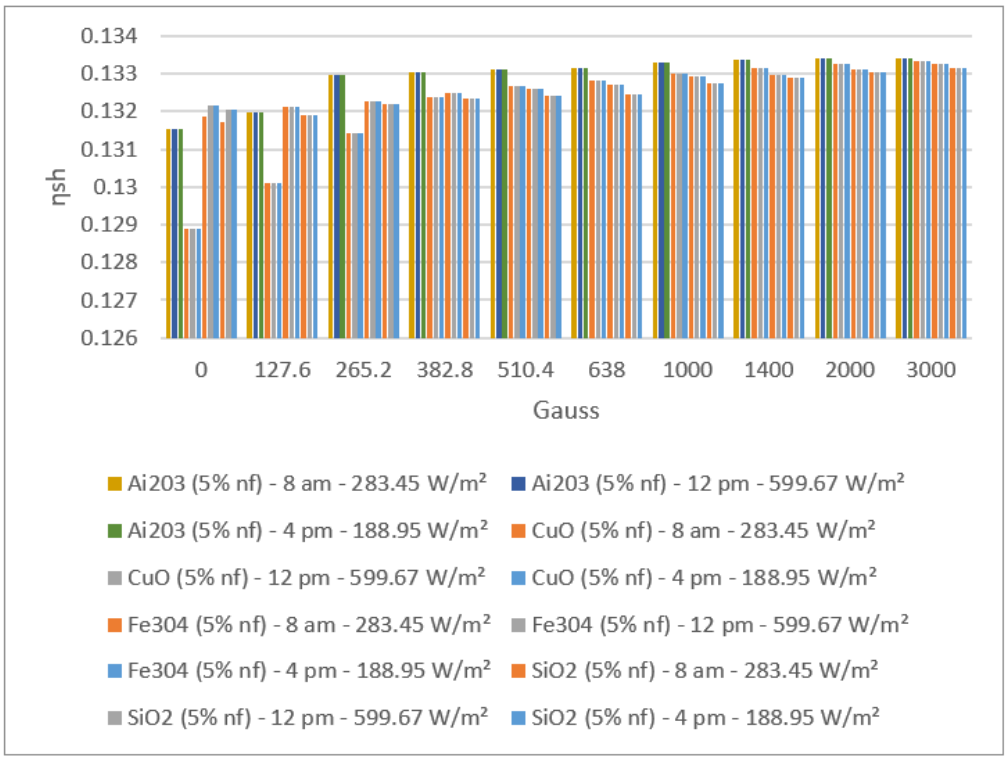

Fig. 13: CSP hybrid efficiency at different magnetic fields

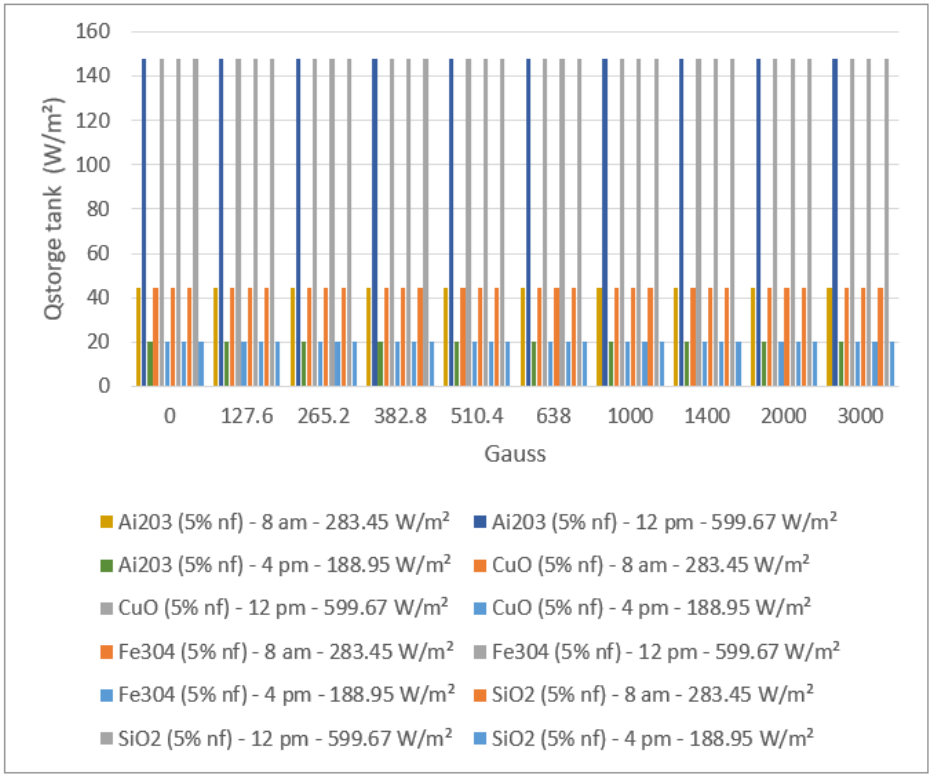

Fig. 14: CSP thermal energy storage at different magnetic fields

The "characteristics of the CSP collector system under solar radiations of 500, 750, 1000 and 1200 w/m^2 occurring at the mid of the day and an angle of incidence of the solar radiation; 77.44° at 12:00 pm and 137.44° have been presented in Fig. 16 through 18. The purpose of this exercise is to predict the impact of a wide range of solar radiations on the characteristics of the CSP collector system. As expected the higher concentrations of the nanofluid AI_2O_3 the more enhanced the characteristics of the CSP collector such as power absorbed and collected, thermal storage energy, the output work at the ORC, over thermal oil as base fluid".

It is noticeable from the results shown in these figures that hat the "ORC key parameters, such as waste heat boiler thermal energy and work produced were enhanced with the increase of the solar radiation and the nanofluid concentrations. It also appears that under magnetized nanofluids concentrations of 5% or less, the CSP characteristics are independent of the concentration. And the magnetized nanofluid Al_2O_3 and CuO have a similar impact on the CSP characteristics. However, the CSP power absorbed and storage tank thermal energy was only enhanced with the solar radiation. It is worthwhile pointing out that nanofluid concentration higher than 20% could result in higher pressure head losses and pumping power losses in the thermal oil loop and that is undesirable. Therefore, the designer of such systems needs to exercise caution when using the Al_2O_3 magnetized nanofluid or other magnetized nanofluids (Sami, 2011; Silva and Castro, 2012; Sharma *et al*., 2017; Sami, 2019a; SRD, 2013; Boonrit, 2017; Sami and Marin, 2019; Sami, 2019b). In particular, Fig. 18 demonstrated, that the CSP system hybrid efficiency, showing that hybrid system efficiency was mainly enhanced by the increase of the solar radiation and at higher nanofluid AI_2O_3 concentrations over the thermal oil as base fluid. Similar results have been observed for the other magnetized nanofluids under investigation."

The data presented in Fig. 16–19 illustrated that "thermal energy stored in the storage tank was enhanced with the increase of solar radiation. This can be interpreted in light of Eq. (1)-(8), where the ORC refrigerant flow increases and consequently the ORC work is produced".

Model Validation

We compared the present "model's prediction of the enhancement ratio of the ORC work produced due to the use of the nanofluids CuO with the data reported by Bellos and Tzivanidis (Bellos *et al*., 2016) that are among the limited experimental data that have been reported in the literature on the use of nanofluids in CSP solar collectors, this comparison is presented in Fig. 20 under nanofluid concentrations of 1-6%. The objective of the Bellos and Tzivanidis work was to optimize and

evaluate a solar-driven trigeneration system that uses nanofluid-based parabolic trough solar collectors. The trigeneration system was studied by Bellos *et al*. (2016) and included an Organic Rankine Cycle (ORC) and an absorption heat pump operating with LiBr-H_2O, which is powered by the heat dissipated from the condenser of the ORC. The comparison between the data of Saadatfar *et al*. (2014) and our model's prediction was conducted for the nanofluids CuO and was based on the enhancement of the work produced by the ORC with nanofluid CuO. It was found that the comparison results from data displayed in Fig. 20 that the model has the same trend; however, some discrepancies existed between the model's prediction and the experimental data. It is believed that the selection of the basic operating parameters: The pressure in the turbine inlet, the temperature in the ORC condenser, and the nanofluid concentration attributed to the discrepancies between the model's prediction and the data. In addition, (Bellos *et al*., 2016) did not disclose the aforementioned parameters, which are critical in the validation of the current model. Therefore, other references were consulted (HTFDC, 2022; Czaplicka *et al*., 2021; Xu *et al*., 2015)".

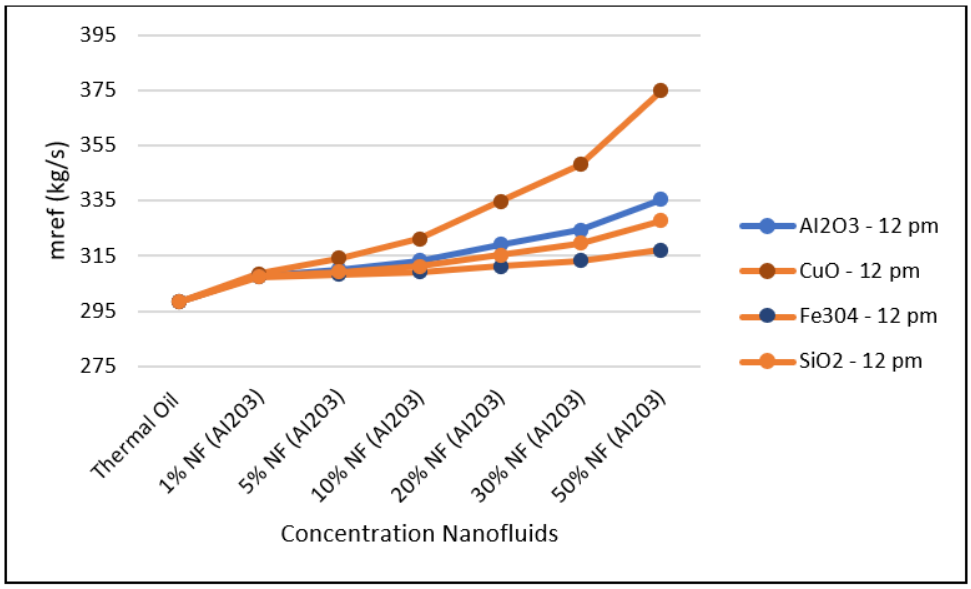

Fig. 15: ORC refrigerant flow rate at different concentrations at different nanofluids

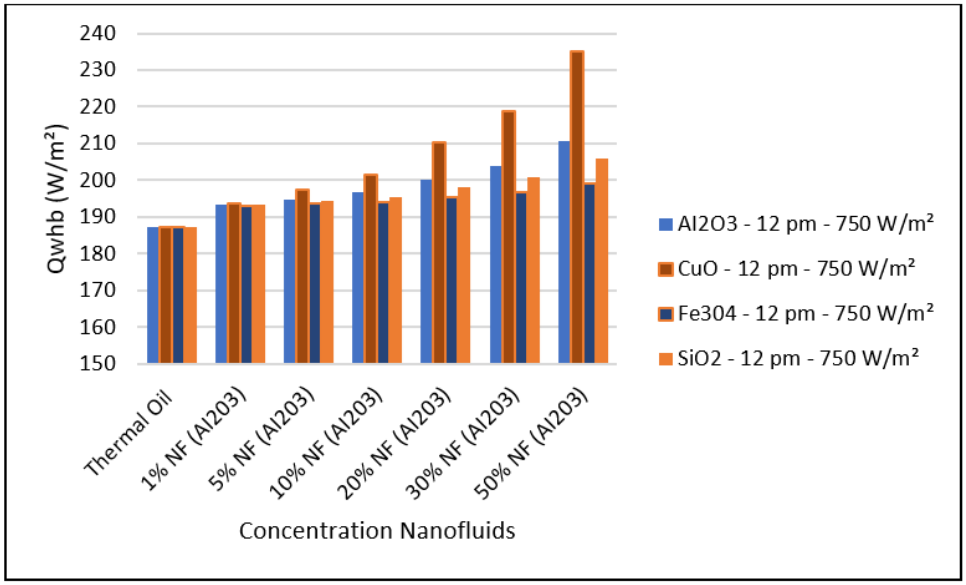

Fig. 16: CSP system hybrid ORC waste heat boiler with different nanofluids at different concentrations

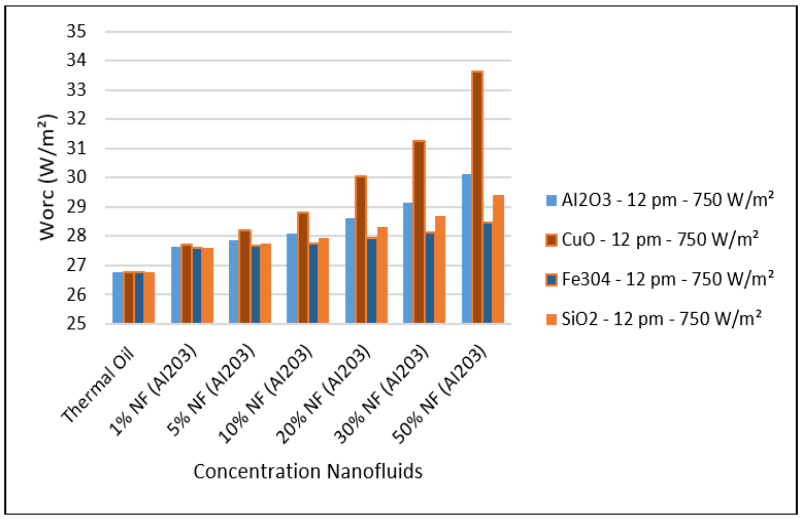

Fig. 17: CSP system hybrid ORC work produced with different nanofluids at different concentrations

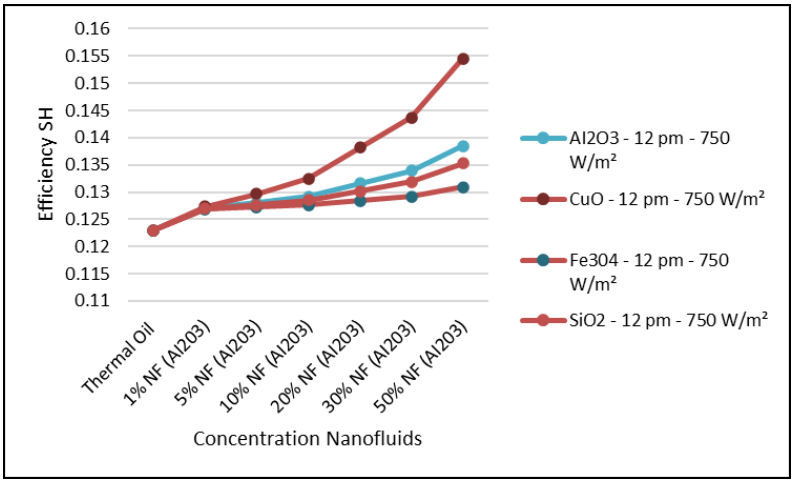

Fig. 18: CSP system hybrid efficiency with different nanofluids at different concentrations

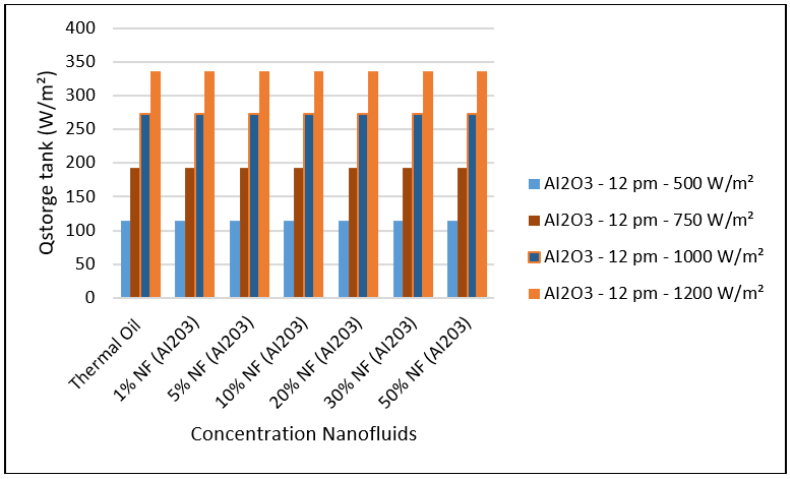

Fig. 19: Thermal energy is stored in the thermal tank at different concentrations of AI_2O_3

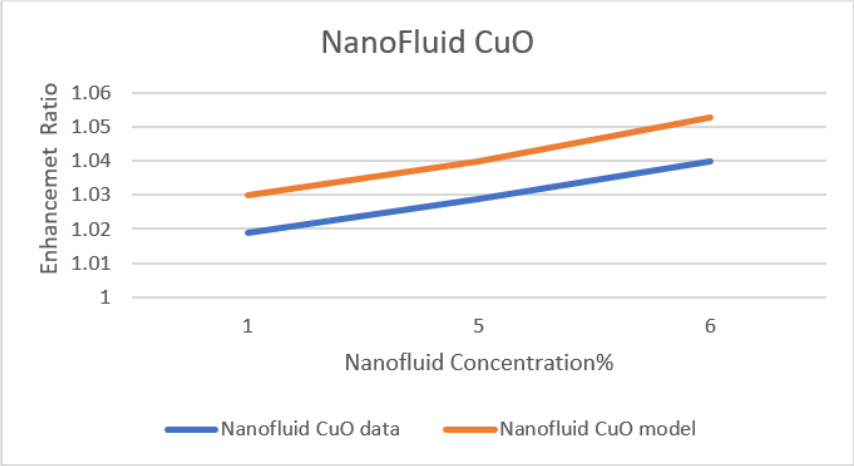

Fig. 20: Comparison between model and data of Bellos and Tzivanidis (2017)

Conclusion

This study is intended to investigate the "enhancement effect and characteristics of nanofluids AI_2O_3, CuO, Fe_3O_4 and SiO_2 in an integrated Concentrating Solar Power (CSP) with ORC and TES under different solar radiations, angle of incidence and different nanofluids concentrations. During this study, the results showed that the power absorbed and power collected by the CSP collector, thermal energy stored in the storage tank, and work produced by the ORC is enhanced with the increase in solar radiation. The results of the efficiencies of the CSP and the hybrid system also showed clearly that the CSP efficiency is higher than the hybrid system efficiency and peaked at midday. It was also found that the CSP hybrid system efficiency was enhanced mainly by the increase of solar radiation and higher nanofluid concentrations over the thermal oil as base fluid. As expected, the results indicate that the higher efficiencies of the hybrid system the higher the solar radiations, but the CSP collector efficiencies are independent of the nanofluid concentrations. In addition, the study concludes that the nanofluid CuO outperforms other nanofluids AI_2O_3, Fe_3O_4, and SiO_2 and has the highest CSP solar collector performance compared to the other nanofluids and thermal oil base fluid under similar conditions. Finally, it was found that the model's prediction compares fairly with data reported in the literature; however, some discrepancies exist between the model's prediction and the experimental data. It is recommended that further experimental studies be conducted using nanofluids AI_2O_3 and SiO_2 in the CSP solar collector loop to obtain more experimental data on the parameters; work enhancement ratios and heat transfer coefficient presented in the validation section under different solar radiation and heat transfer fluid different conditions. This should help to tune the model and improve the predicted results".

Acknowledgment

The research work presented in this study was made possible by the help of Edwin Martin in executing the numerical calculations.

Nomenclature

C_{poil}	Specific heat of thermal oil the base fluid
DNI	Solar radiation (w/m^2)
E_l	End losses
h_1	Enthalpy at the outlet of the waste heat boiler (kj/Kg)
h_2	Enthalpy at the exit of the vapor turbine (kj/Kg)
h_3	Enthalpy at the condenser outlet (kj/kg)
h_4	Enthalpy at ORC pump outlet (kj/kg)
m_{ref}	Refrigerant mass flow rate (kg/s)
m_{oil}	Is the oil flow rate obtained from Equation (8)
IAM	Incidence angle modifier.
P_{abs}	Collector power absorbed by CSP defined in Eq. (1)
$P_{losscol}$	Collector thermal losses of the CSP
$P_{losspip}$	Solar field piping losses
R_s	Row shadow
SF_{Aval}	Solar field available
Greek	
Θ	Angle of incidence
η_{opt}	Optical efficiency
ρ_p	Represents the density of the nanoparticle

Ethics

This article is original and contains unpublished material. The corresponding author confirms that all of the other authors have read and approved the manuscript and no ethical issues are involved.

References

Alashkar, A., & Gadalla, M. (2018, June). Thermodynamic Analysis of a Parabolic Trough Solar Collector Power Generation Plant Coupled With an Organic Rankine Cycle. In ASME Power Conference (Vol. 51395, p. V001T06A030). American Society of Mechanical Engineers. doi.org/10.1115/POWER2018-7548

Bahram, S., Reza, F., & Fransson, T. (2013). Waste heat recovery Organic Rankine cycles in sustainable energy conversion: A state-of-the-art review. The Journal of MacroTrends in Energy and Sustainability, 1(1), 161-188. https://www.diva-portal.org/smash/record.jsf?pid=diva2%3A1313002&dswid=-1027

Bellos, E., & Tzivanidis, C. (2017). Optimization of a solar-driven trigeneration system with nanofluid-based parabolic trough collectors. Energies, 10(7), 848. doi.org/10.3390/en10070848

Bellos, E., Tzivanidis, C., & Antonopoulos, K. A. (2016). Exergetic, energetic and financial evaluation of a solar-driven absorption cooling system with various collector types. Applied Thermal Engineering, 102, 749-759. doi.org/10.1016/j.applthermaleng.2016.04.032

Boonrit, P. (2017). Efficiency improvement of a concentrated solar receiver for water heating system using a porous medium. IOP Conf. Ser. Mater. Sci. Eng. 2017, 297, 012059. doi.org/10.1088/1757-899X/297/1/012059

Bozorgan, N., & Shafahi, M. (2015). Performance evaluation of nanofluids in solar energy: A review of the recent literature. Micro and Nano Systems Letters, 3(1), 1-15. doi.org/10.1186/s40486-015-0014-2

Calise, F., & Vanoli, L. (2012). Parabolic trough photovoltaic/thermal collectors: Design and simulation model. Energies, 5(10), 4186-4208. doi.org/10.3390/en5104186

Czaplicka, N., Grzegórska, A., Wajs, J., Sobczak, J., & Rogala, A. (2021). Promising nanoparticle-based heat transfer fluids-environmental and techno-economic analysis compared to conventional fluids. International Journal of Molecular Sciences, 22(17), 9201. doi.org/10.3390/ijms22179201

Dickes, R., Dumont, O., Declaye, S., Quoilin, S., Bell, I., & Lemort, V. (2014). Experimental investigation of an ORC system for a micro-solar power plant. https://docs.lib.purdue.edu/icec/2372/

Freeman, J., Guarracino, I., Kalogirou, S. A., & Markides, C. N. (2017). A small-scale solar organic Rankine cycle combined heat and power system with integrated thermal energy storage. Applied thermal engineering, 127, 1543-1554. doi.org/10.1016/j.applthermaleng.2017.07.163

HTFDC. (2022). Heat Transfer Fluid-Dow Chemical. https://www.dow.com/webapps/lit/litorder.asp?filepath=/heattrans/pdfs/noreg/176

Iacobazzi, F., Milanese, M., Colangelo, G., Lomascolo, M., & de Risi, A. (2016). An explanation of the Al2O3 nanofluid thermal conductivity based on the phonon theory of liquid. Energy, 116, 786-794. doi.org/10.1016/j.energy.2016.10.027

Incropera, F., & DeWitt, D. (1994) Fundamentals of Heat and Mass Transfer, 4th ed.; Wiley: New York, NY, USA, 1994; p. 493, ISBN-10: 978-0-471-30460-9.

Islam, M. T., Huda, N., Abdullah, A. B., & Saidur, R. (2018). A comprehensive review of state-of-the-art Concentrating Solar Power (CSP) technologies: Current status and research trends. Renewable and Sustainable Energy Reviews, 91, 987-1018. doi.org/10.1016/j.rser.2018.04.097

Izquierdo, S., Montanes, C., Dopazo, C., & Fueyo, N. (2010). Analysis of CSP plants for the definition of energy policies: The influence on electricity cost of solar multiples, capacity factors, and energy storage. Energy Policy, 38(10), 6215-6221. doi.org/10.1016/j.enpol.2010.06.009

Lomascolo, M., Colangelo, G., Milanese, M., & De Risi, A. (2015). Review of heat transfer in nanofluids: Conductive, convective, and radiative experimental results. Renewable and Sustainable Energy Reviews, 43, 1182-1198. doi.org/10.1016/j.rser.2014.11.086

Macchi, E., & Astolfi, M. (Eds.). (2016). Organic Rankine Cycle (ORC) power systems: Technologies and applications. Woodhead Publishing. doi.org/10.1016/B978-0-08-100510-1.00016-8

Marefati, M., Mehrpooya, M., & Shafii, M. B. (2018). Optical and thermal analysis of a parabolic trough solar collector for production of thermal energy in different climates in Iran with a comparison between the conventional nanofluids. Journal of cleaner production, 175, 294-313. doi.org/10.1016/j.jclepro.2017.12.080

Milanese, M., Colangelo, G., Cretì, A., Lomascolo, M., Iacobazzi, F., & De Risi, A. (2016). Optical absorption measurements of oxide nanoparticles for application as nanofluid indirect absorption solar power systems–Part I: Water-based nanofluids behavior. Solar Energy Materials and Solar Cells, 147, 315-320. doi.org/10.1016/j.solmat.2015.12.030

Mohamad, A., Orfi, J., & Alansary, H. (2014). Heat losses from parabolic through solar collectors. International journal of energy research, 38(1), 20-28. doi.org/10.1002/er.3010

Nagarajan, P. K., Subramani, J., Suyambazhahan, S., & Sathyamurthy, R. (2014). Nanofluids for solar collector applications: A review. Energy Procedia, 61, 2416-2434. doi.org/10.1016/j.egypro.2014.12.017

Paces, S. (2016). CSP Projects around the world. IEA. Solar Power and Chemical Energy Systems.

Pavlović, T. M., Radonjić, I. S., Milosavljević, D. D., & Pantić, L. S. (2012). A review of concentrating solar power plants in the world and their potential use in Serbia. Renewable and Sustainable Energy Reviews, 16(6), 3891-3902. doi.org/10.1016/j.rser.2012.03.042

Peters, M., Schmidt, T. S., Wiederkehr, D., & Schneider, M. (2011). Shedding light on solar technologies-A techno-economic assessment and its policy implications. Energy Policy, 39(10), 6422-6439. doi.org/10.1016/j.enpol.2011.07.045

Saadatfar, B., Fakhrai, R., & Fransson, T. (2014). Conceptual modeling of nanofluid ORC for solar thermal polygeneration. Energy Procedia, 57, 2696-2705. doi.org/10.1016/j.egypro.2014.10.301

Saloux, E., Sorin, M., Nesreddine, H., & Teyssedou, A. (2019). Thermodynamic Modeling and Optimal Operating Conditions of Organic Rankine Cycles (ORC) Independently of the Working Fluid. Int. J. Green Technol, 5, 9-22. doi.org/10.30634/2414-2077.2019.05.02

Sami, S. (2019a). Analysis of nanofluids behavior in concentrated solar power collectors with organic Rankine cycle. Applied System Innovation, 2(3), 22. doi.org/10.3390/asi2030022

Sami, S. (2019b). Impact of magnetic field on the enhancement of performance of thermal solar collectors using nanofluids. Int. J. Ambient Energy 2019, 40, 1–10, doi.org/10.1080/01430750.2018.1437561

Sami, S. M. (2011). The behavior of ORC low-temperature power generation with different refrigerants. International Journal of Ambient Energy, 32(1), 37-45. doi.org/10.1080/01430750.2011.584451

Sami, S., & Marin, E. (2016). A numerical model for predicting the dynamic performance of biomass-integrated Organic Rankine Cycle (ORC), System for Electricity Generation. AJEE Am. J. Energy Eng, 4, 26-33. doi.org/10.11648/j.ajee.20160403.11

Sami, S., & Marin, E. (2019). Modeling and simulation of PV solar-thermoelectric generators using nanofluids. International Journal of Sustainable Energy and Environmental Research, 8(1), 70-99. doi.org/10.18488/journal.13.2019.81.10.28

Sharma, K. V., Akilu, S., Hassan, S., Hegde, G. (2017) Considerations on the Thermophysical Properties of Nanofluids. In Engineering Applications of Nanotechnology, Topics in Mining, Metallurgy and Materials Engineering; Springer: Berlin, Germany, 2017, doi.org/10.1007/978-3-319-29761-3_2

Shin, D., Jo, B., Kwak, H. E., & Banerjee, D. (2010, January). Investigation of high-temperature nanofluids for solar thermal power conversion and storage applications. In International Heat Transfer Conference (Vol. 49422, pp. 583-591). doi.org/10.1115/IHTC14-23296

Silva, J. A. P., & Castro, R. (2012). Modeling and Simulation of a Parabolic Trough Power Plant. doi.org/10.1515/green-2011-0019

SRD. (2013). Standard Reference Data. https://www.nist.gov/srd/refprop

Taylor, R. A., Phelan, P. E., Otanicar, T. P., Walker, C. A., Nguyen, M., Trimble, S., & Prasher, R. (2011). Applicability of nanofluids in high flux solar collectors. Journal of Renewable and Sustainable Energy, 3(2), 023104. doi.org/10.1063/1.3571565

Tzivanidis, C., Bellos, E., & Antonopoulos, K. A. (2016). Energetic and financial investigation of a stand-alone solar-thermal Organic Rankine Cycle power plant. Energy conversion and management, 126, 421-433. doi.org/10.1016/j.enconman.2016.08.033

Ummadisingu, A., & Soni, M. S. (2011). Concentrating solar power–technology, potential, and policy in India. Renewable and sustainable energy reviews, 15(9), 5169-5175. doi.org/10.1016/j.rser.2011.07.040

Wang, R., Jiang, L., Ma, Z., Gonzalez-Diaz, A., Wang, Y., & Roskilly, A. P. (2019). Comparative analysis of small-scale organic Rankine cycle systems for solar energy utilization. Energies, 12(5), 829. doi.org/10.3390/en12050829

Xu, Z. Y., Wang, R. Z., & Wang, H. B. (2015). Experimental evaluation of a variable effect LiBr–water absorption chiller designed for a high-efficient solar cooling system. International Journal of Refrigeration, 59, 135-143. doi.org/10.1016/j.ijrefrig.2015.07.019

Zhang, X., Wu, Y., Ma, C., Meng, Q., Hu, X., & Yang, C. (2019). Experimental study on temperature distribution and heat losses of a molten salt heat storage tank. Energies, 12(10), 1943. doi.org/10.3390/en12101943